Fourier Transform Rheometry on Gum Elastomers

Jean L. Leblanc

University P. & M. Curie (Paris 6), Polymer Rheology and Processing, 60, Rue Auber, F-94408 Vitry sur Seine, France

Received 2 August 2002; accepted 30 September 2002

ABSTRACT: Using a modified torsional dynamic rheometer, strain and torque signals are captured and analyzed through Fourier transform. A thorough analysis of strain signal is first performed to document the quality of the applied deformation and to define the optimum conditions for signal capture, and hence, for Fourier transform calculation. A specific calculation procedure is developed that allows the error associated with FT calculation to be estimated, in terms of mean harmonic peaks and their standard deviation. Scatter is observed on low strain results that nearly vanishes when the applied deformation is larger than 14%, thus giving confidence in data gathered under nonlinear viscoelastic conditions. Results on a series of gum EPDM with different macromolecular characteristics (MWD and long chain branching, LCB) are reported and discussed, with respect to a simple four parameters model for the variation on deformation of the relative third harmonic component. Processing additives are found to mask expected LCB effects. Results on a series of SBR 1500 samples, collected from various manufacturers, are presented that illustrate the capability of FT rheometry to detect differences between materials expected to be similar. © 2003 Wiley Periodicals, Inc. J Appl Polym Sci 89: 1101–1115, 2003

Key words: elastomers; rheology; viscoelastic properties; branched; structure–property relations

INTRODUCTION

Fourier transform rheometry is an emerging new technique that allows the linear and nonlinear viscoelastic behavior of polymer materials to be accurately investigated. Essentially, the method consists in submitting samples to torsional harmonic strain at fixed frequency and temperature to capture the full strain and torque signals. Fourier transform is then applied to captured signals to resolve them in their main component and other harmonics, if any. Contrary to standard dynamic testing methods whose validity in extracting the elastic and viscous components from the (measured) complex torque is limited to the linear viscoelastic range, Fourier transform rheometry provides valid results, whatever the response of the tested material, even in the far nonlinear range.

Any dynamic rheometer can be suitably modified for Fourier transform rheometry, as illustrated by the pioneering works of M. Wilhelm,[1] but most cone-and-plate or parallel-plates instruments do not yield good results with very stiff materials, such as elastomers and their compounds, essentially because wall slip and other perturbating effects occur when large amplitude oscillatory strains are applied. Special instruments are needed for rubber materials and a commercial one, i.e., the Rubber Process Analyzer RPA 2000, was suitably modified for Fourier transform rheometry. Details of the modification were previously reported,[2] and the present work is a sequel of this development.

The aims of this article are first to present a detailed analysis of RPA strain signal with the objectives to document the quality of the applied deformation and to define the optimum conditions for signal capture, and hence, for Fourier transform calculation. Then results on a series of gum EPDM with different macromolecular characteristics (MWD and branching) will be reported and analyzed. Eventually results on a series of SBR 1500 samples, collected from various manufacturers, will be presented.

ANALYZING RPA STRAIN SIGNAL THROUGH FOURIER TRANSFORM

Ideal vs. practical dynamic testing

In ideal dynamic testing, a perfect sinusoidal deformation at controlled frequency and strain must be applied on test material. In practice, however, there are technical limits in accurately producing any harmonic mechanical motion and, in what dynamic testing is concerned, other difficulties arise depending on the method used to transfer the harmonic displacement to the material under testing. With viscoelastic fluids, most dynamic methods have some analogy with drag flow experiments, i.e., the (harmonic) probing of the material results from an excitation by means of a vibrating rigid body, for instance, the cone in a cone-and-plate device, or the upper die in the RPA. The quality of the harmonic displacement applied to

Journal of Applied Polymer Science, Vol. 89, 1101–1115 (2003)

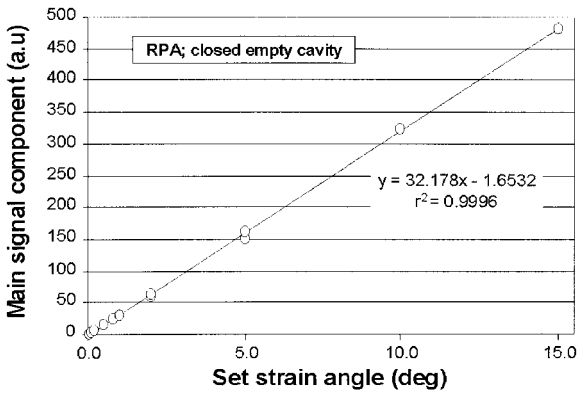

Figure 1 Analyzing RPA strain capabilities through FT analysis; empty cavity.

the vibrating body is, of course, depending on the care taken by the manufacturer in designing and building the instrument, but because no easy facility is provided to check it, the quality of the applied signal is often taken for granted. Fast Fourier transform of the strain (i.e., applied) signal allows this aspect to be easily documented, but FT spectra must also be considered with respect to specific aspects of the test device.

In developing an experimental set up for FT-rheology experiments, Wilhelm[1] has modified and extended a commercial ARES-rheometer from Rheometric Scientific. This instrument is a cone-and-plate rheometer designed for accurate experiments on viscoelastic materials in an ideal laboratory environment. Through careful calibration experiments, Wilhelm demonstrated that there is a nonlinear contribution from the instrument in the range of 10^{-3} to 10^{-4} relative to the response at the excitation frequency. No major influence from the apparatus is thus expected within an error of 0.1% relative intensity, Wilhelm concluded. In another publication,[3] the same author demonstrated that the shear geometry, either cone-and-plate or parallel plates, affects the degree of nonlinear behavior as characterized by the ratio of the third harmonic $I(3\omega_1)$ to the fundamental frequency $I(\omega_1)$. In the linear regime, the expected difference between the two geometries can be considered by using an appropriate shift factor of 0.75, based on the concept of a characteristic radius for the parallel plate geometry.[4] When applying this factor to $I(3\omega_1)/I(\omega_1)$ ratios derived from FT on parallel plate data, the discrepancies between nonlinear experiments with the two geometries is somewhat reduced, but the results still depend on the test gap in the strongly nonlinear regime.

With respect to the RPA operating mode, an effect of the test geometry could also be expected and, because the device uses a closed cavity in which the material is maintained under pressure, larger nonlinear instrumental contributions are possible. The RPA is a robust instrument, designed for easy loading and operation in factory like conditions but, owing to its design, it allows very stiff materials (e.g., filled rubber compounds) to be tested in a reproducible manner; a performance not possible with cone-and-plate instruments.

Analyzing RPA strain signal when cavity is empty

The quality of RPA test capabilities was documented by estimating the nonlinear contribution from the instrument through strain signal analysis by Fourier transform. A series of strain signals were first captured by running the empty cavity of the RPA under various strain angle (0.05 to 15.0 deg) and either 0.1 or 1.0 Hz frequency conditions. No significant torque signal was of course obtained. For each test conditions, 10,240 points were acquired and the last 4096th ones ($= 2^{12}$) were used to extract the Fourrier transform spectra of the harmonic motion of the lower die. As expected, a linear relationship is observed between the set strain angle and the main strain component revealed by FT analysis (Fig. 1), and no influence of the frequency is noted.

The quality of the strain angle produced by the RPA is adequately checked through the relative harmonic components, i.e., $I(n\omega_1)/I(\omega_1)$ ratio (%). As shown in Figure 2, whatever the set strain or the frequency, the common pattern emerged of a third harmonic contribution of 1.5 $\pm$ 0.8% of the main strain component, a fifth harmonic contribution of 0.9 $\pm$ 0.6%, and the subsequent harmonics contributing for less than 0.5 $\pm$ 0.3%. The strain signal provided by the RPA can, therefore, be considered as of excellent quality.

Analyzing RPA strain signal with fully loaded cavity

A special aspect of RPA design is that the cavity thickness is not directly controlled but expected to be

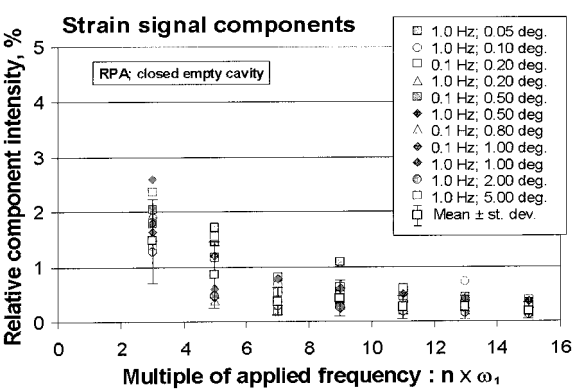

Figure 2 Harmonic components of RPA strain signal; empty cavity.

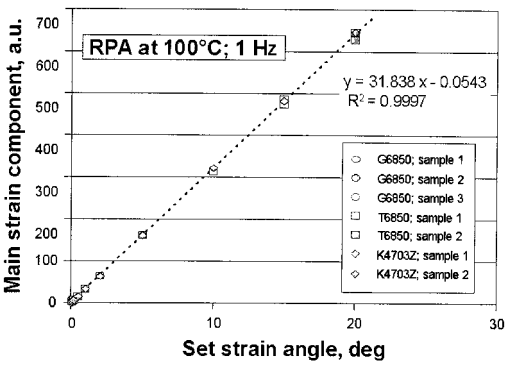

Figure 3 Analyzing RPA strain capabilities through FT analysis; loaded cavity.

in the 0.5-mm range through the application of the cavity closure pressure and the correct excess volume for the test sample. When using the instrument in standard operating modes, it was demonstrated that such a design does not significantly affect the validity and the reproduciblity of the measurements.[5] However, a slight retroactive effect due to the test material in the cavity cannot be excluded as a source of additional nonlinear contribution to the instrument, that would likely scatter the recorded torque signal.

To check this aspect, a series of strain sweep tests at 1 Hz were performed at 100°C on several EPDM samples. Test samples were die-cut from 1.5 cm-thick slices directly cut from the bale; no particular care was given to sample shape (whose cross-section was circular) but the sample weight was maintained within a 3.05 ± 0.04 g range. Strain signals were recorded and analyzed through Fourier transform.

Figure 3 shows that the direct proportionality between the set strain angle, and the main strain component is nearly perfect and compares well with the similar observation made when running the RPA cavity empty.

The quality of the strain signal is considered through the relative third harmonic component, as shown in Figure 4. As can be seen, the larger the strain angle, the lower the relative third component; in other words, the larger the applied strain, the "purer" the signal. At first sight, the sample nature seems to play a role but the enlargement obtained when using a logarithm scale for the set strain shows no such effect. The scatter on $S(3\omega_1)/S(\omega_1)$ ratio begins to reduce to ±1.0% when the set strain is 0.5 deg (6.98% deformation) and further decreases above this strain angle. Note that in this article, $I(n\omega_1)/I(\omega_1)$ or the abridged form *I(n/1)*, is used to describe the n^{th} relative harmonic component of any harmonic signal; $S(n\omega_1)/S(\omega_1)$ specifically means that a Strain signal is considered; $T(n\omega_1)/T(\omega_1)$ is used for the Torque signal. The lowest strain angle for good quality applied strain is thus 0.5 deg. (which, in fact, meets manufacturer's recommendations). Below this value, erratic effects superimpose to the intrinsic nonlinear contribution from the instrument, which likely affect excessively the measured viscoelastic response of the tested material.

APPLYING FAST FOURIER TRANSFORM

Optimizing data acquisition

The RPA was modified in such a manner that both the strain and torque signals are readily captured and made available as data files of actual harmonic strain and stress readings vs. time.[2] The PC-card used to capture the data has a resolution of 16 bits with a maximum sampling rate of around 205 K sample/second. The data acquisition protocol is generally as follows: first, the actual test conditions in terms of temperature, frequency, and strain angle are selected through the built-in capabilities of the instrument, then a sample is positioned on the lower die, and the cavity is closed. After a sufficient warmup time, generally 3 to 5 min, the selected test is started and the data acquisition system is manually activated. The data acquisition runs until the selected number of data points have been recorded, with respect to the selected acquisition parameters used.

The size of the data file is an obvious aspect in selecting the optimum number of acquired data points but not the most important one. First, a steady harmonic regime must be reached before suitable data points needed for Fourier transform are obtained. Indeed, as pointed out by Nelson and Dealy,[6] there are always startup transients in the input strain that are causing some aperiodicity in the measured stress signal, at the start of the test. Several cycles are needed before the initial transients become negligible. Second, most common FFT algorithms require 2^n data points, and the value of n is a compromise between the size of the data file (for instance, a 3 columns × 10,000 rows file correspond to some 300 Kilo-octet), and the num-

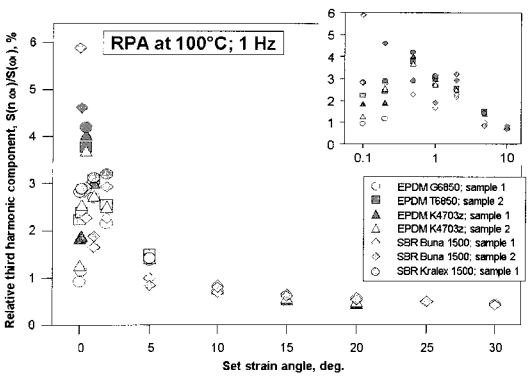

Figure 4 Third harmonic component of applied strain signal; RPA loaded cavity.

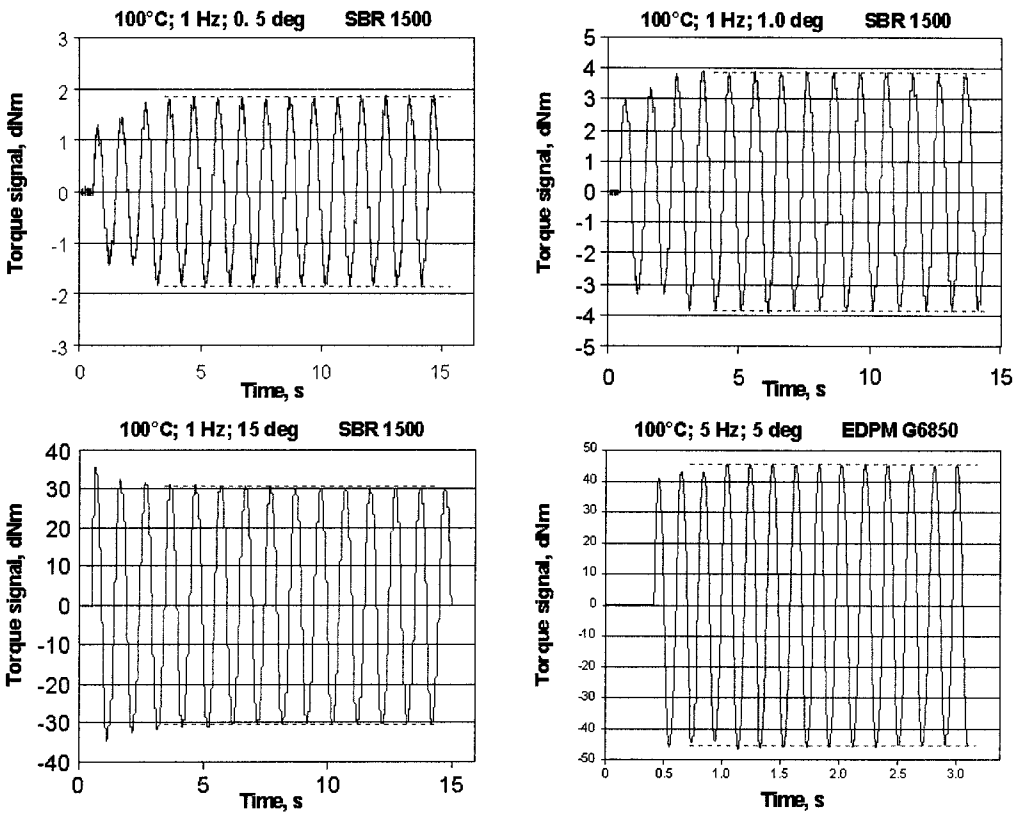

Figure 5 Start-up transient torque signals as measured with a modified RPA.

ber of necessary acquired data to optimize the signal-to-noise (S/N) ratio. By experience, $n = 12$ (i.e., 4096 data points) was found appropriate, providing such points correspond to the steady harmonic response of the material. Depending on the material and on the test conditions (temperature, frequency, and strain) the steady harmonic response is obtained more or less quickly, as illustrated in Figure 5, but the last cycles reflect generally a "dynamic steady state." A close examination of the figure reveals, however, that there is some scatter in the extrema of the recorded torque signal, likely affecting the Fourier transform calculation.

A third important aspect in setting the data acquisition parameters is related to the concepts of sampling period (so-called "dwell time" in Wilhelm's publications), spectral width and resolution. The *dwell time* t_d (s) is the time interval between two data points digitized from the continuous signal by the analog-to-digital converter. The *sampling frequency* (or rate) f_s (point/second, pt/s) is obviously the reverse of the dwell time, and for N acquired data points, the acquisition time t_a is equal to $t_d \times N$. The *spectral width* is the highest frequency that can be resolved (by the Fourier transform) at a given sampling rate; this quantity, also called the Nyquist frequency f_{Nyq}, is defined as:

$$f_{Nyq} = \frac{1}{2t_d} = \frac{1}{f_s}.$$

The *spectral resolution* is the reverse of the acquisition time, and is the frequency difference between two points of the spectrum obtained by Fourier transform. If a signal contains components with frequencies above f_{Nyq}, they are reflected back into the frequency domain below. A disturbance can thus be expected owing to the power line (50 Hz in Europe) if the sampling frequency is lower that 50 Hz. Finally, discrete Fourier transform algorithms assume that the window of sampled data is periodic, and therefore, care must be taken to ensure that an integral number of cycles is sampled.[6] By combining all these requirements, optimal data acquisition parameters were defined to capture 10,240 points per test, i.e., $2^{11} + 2 \times 2^{12}$ points or $2048 + 2 \times 4096$ points, enough data to run the FT algorithm either on 4096 (2^{12}) or on 8192 (2^{13}) points, with provision for ensuring a steady harmonic signals (the first 2048 points). Having fixed the number of data points ($N = 10240$), the acquisition frequency f_s is then selected with respect to the test frequency f_t and a reasonnable acquisition time t_a, using the following equality: $N = f_t \times f_a \times t_a$. Table I gives typical data acquisition parameters (for 10,240 data points, pt) for experiments with the modified RPA.

Compensating experimental scatter

Even when the steady harmonic regime is reached, the recorded sinusoids still exhibit some scatter. To some-

TABLE I
Setting Data Acquisition Parameters (for 10,240 Data Points)

Test freq., f_t (Hz)	Acq. freq., f_a (pt/s)	Acq. time, t_a (s)	Dwell Time, t_d (s)	Number of cycles
0.1	1280	80	0.00781	8
0.2	640	80	0.00781	16
0.4	160	160	0.01563	64
0.8	80	160	0.01563	128
1.0	512	20	0.00195	20
2.0	256	20	0.00195	40
10.0	128	8	0.00078	80

what compensate this effect, the Fourier transform is first performed using the last 4096 points of the data set, then the calculation is repeated on the same number of points but read at several back positions in the data set. For instance, using a 10,240 points data set, FT is performed with points 6144 to 10,240, then with points 6080 to 10,176, then 6016 to 10,112, etc. FT spectra obtained are then averaged and the standard deviations calculated. A specific calculation programme was written using the Fourier transform algorithm available in Mathcad 8.0® (MathSoft Inc.), to obtain the amplitude of the main stress and strain components (corresponding the test frequency) and the relative magnitudes (in %) of the odd-harmonic components, i.e. $I(n \times \omega_1)/I(\omega_1)$. The number of data points used, the frequency resolution (Hz), the acquisition time (s), and the sampling rate (point/s) are also displayed. Figure 6 shows the single Fourier transform spectrum obtained when analyzing the last 4096 points of the signals recorded when submitting an EDPM sample to 2 deg dynamic strain at 1 Hz. The results of the odd harmonic components analysis are displayed in the inserted table. Table II gives the results of the full calculation procedure, on five sets of data points, to obtain mean torque and strain components, with their corresponding standard deviations.

As can be seen, the results of the Fourier transform analysis are well reproducible when different sets of 2^{12} points are considered from the signal sampling. Mean torque and strain data are obtained with their respective standard deviations. Up to the fifth harmonic, the scatter is less than 0.01 of the $I(n\omega_1)/I(\omega_1)$ ratio, and even lower for higher harmonic components.

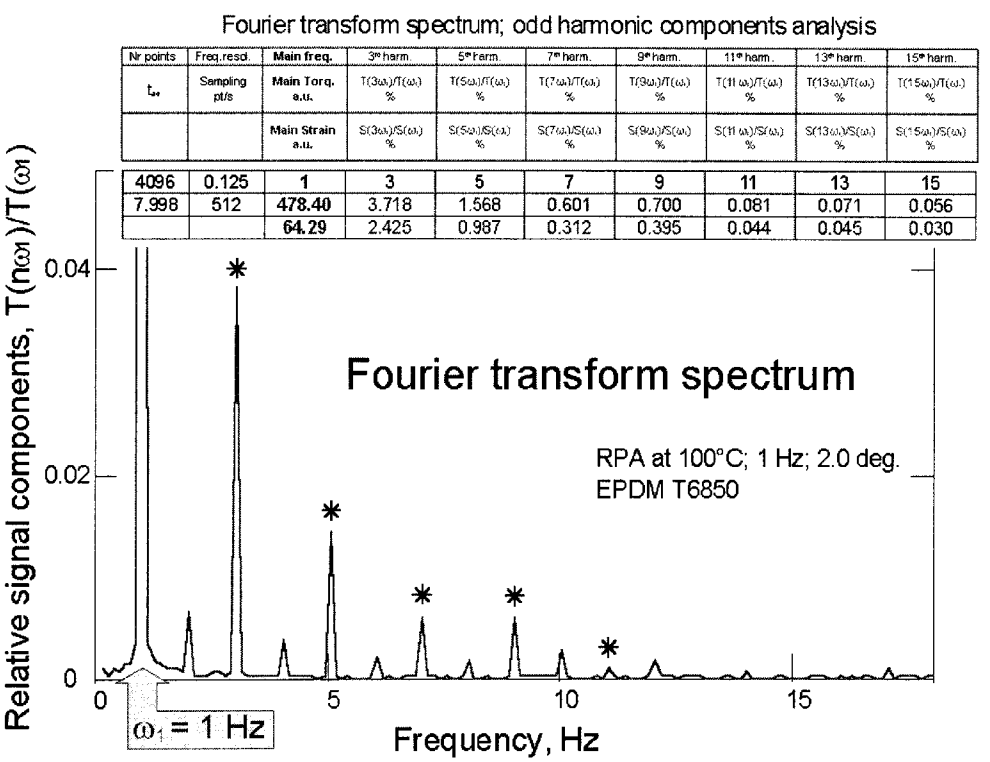

Figure 6 Fourier transform spectrum and analysis of odd-harmonic components.

TABLE II
Fourier Transform-Analysis

Freq. (Hz):	1	3rd harm.	5th harm.	7th harm.	9th harm.	11th harm.	13th harm.	15th harm
Data point set	$I(\omega_1)$	$\frac{I(3\omega_1)}{I(\omega_1)}$	$\frac{I(5\omega_1)}{I(\omega_1)}$	$\frac{I(7\omega_1)}{I(\omega_1)}$	$\frac{I(9\omega_1)}{I(\omega_1)}$	$\frac{I(11\omega_1)}{I(\omega_1)}$	$\frac{I(13\omega_1)}{I(\omega_1)}$	$\frac{I(15\omega_1)}{I(\omega_1)}$
	a.u	%	%	%	%	%	%	%
6144 to 10240	478.40	3.718	1.568	0.601	0.700	0.081	0.071	0.056
	64.29	2.425	0.987	0.312	0.395	0.044	0.045	0.030
6080 to 10176	478.30	3.704	1.582	0.591	0.699	0.085	0.069	0.063
	64.28	2.388	1.010	0.301	0.399	0.054	0.037	0.031
6016 to 10112	478.20	3.698	1.552	0.594	0.709	0.081	0.072	0.060
	64.29	2.400	0.977	0.308	0.402	0.044	0.047	0.032
5888 to 9984	478.40	3.725	1.562	0.588	0.698	0.080	0.062	0.052
	64.30	2.427	0.986	0.307	0.392	0.043	0.042	0.030
5632 to 9728	478.50	3.727	1.562	0.582	0.698	0.080	0.047	0.049
	64.30	2.424	0.982	0.302	0.390	0.045	0.040	0.034
Torque:								
Mean	478.40	3.714	1.565	0.591	0.701	0.081	0.064	0.056
St.Dev.	0.10	0.012	0.010	0.007	0.004	0.002	0.009	0.005
Strain:								
Mean	64.29	2.413	0.989	0.306	0.395	0.046	0.042	0.031
St.Dev.	0.01	0.016	0.011	0.004	0.004	0.004	0.003	0.001

RPA at 100°C; 1 Hz; 2.0 deg; EPDM T6850.

TESTING GUM EPDM THROUGH FT RHEOMETRY

Ethylene–Propylene–Diene test materials

Three Ethylene–Propylene–Diene monomer terpolymer (EPDM) elastomers were selected to offer comparable ethylene/propylene ratio, ethylene norbornene content, and Mooney viscosity but different degrees of long chain branching (LCB), as described in Table III. There is no direct, undisputable method to measure the (long) chain branching content of a polymer, and it is only the polymerization process, its control, and the catalyst system used that allow manufacturers to assign a qualitative degree of LCB to a given material. Booij has introduced an indirect method, based on torsional dynamic measurements on gum rubber samples.[7] The method consists in measuring the loss angle (δ) over a frequency range of several decades, in the linear viscoelastic region (i.e., at low strain angle) of the material and to consider the difference in phase angle at 10^{-1} and 10^{2} rad/s. This quantity is called the $\Delta\delta$, and is claimed to decrease with the "degree" of long chain branching. The three EPDM samples used rank accordingly with respect to their LCB level.

RPA test protocols

Sample preparation was reduced to minimum, as follows: around 2 cm-thick slices were cut from bale and test samples of circular cross-section were cut with a 18 mm diameter die. Each sample was weighed and, if necessary, adjusted to maintain its weight within 3.05 $\pm$ 0.4 g.

Strain sweep tests were performed with the RPA, according to the protocol described in Table IV. At each strain sweep step, the data acquisition for Fourier transform treatment was made to record 10,240 points at the rate of 512 pt/s. Twenty cycles were consequently recorded at each strain step, with the immediate requirement that the RPA was set to apply a sufficient number of cycles (i.e., 40 cycles; the so-called "stability" condition) for the steady harmonic regime to be reached. The data acquisition was activated as

TABLE III
EPDM Samples

Polymer	Supplier	Ethylene content (wt %)	ENB[a] content (wt %)	Mooney ML(1 + 4) 100°C	MWD[b]	Degree of long chain branching	$\Delta\delta$[c]
Buna EP T 6850	Bayer	51	8	58	Narrow	low	36–43
Buna EP G 6850	Bayer	51	8	62	Medium	medium	31–32.5
Keltan 4703Z	DSM	48	9	64	Broad	high	25–28

[a] Ethylene Norbonene.
[b] Molecular weight distribution.
[c] $\Delta\delta = \delta\lfloor\omega = 10^{-1}$ rad/s$\rfloor - \delta\lfloor\omega = 10^{2}rad/s\rfloor$; RPA, 0.5 deg strain angle, Temp. range: 70 to 125°C.

TABLE IV
RPA; Strain Sweep Test Protocol; 0.1 to 20.0 deg

RPA test conditions	Temp. (°C): 100 Freq. (Hz): 1
Sample conditionning	
Preheating	3 min, at rest
Fixing	30 sec; 1 Hz; 0.05 deg.
Strain sweep test (run 1)	
Dwell time	2 min, at rest
Strain Sweep	0.1; 0.2; 0.5; 1.0; 2.0; 5.0; 10.0; 15.0; 20.0 deg
Strain sweep test (run 2)	
Dwell time	2 min, at rest
Strain Sweep	0.1; 0.2; 0.5; 1.0; 2.0; 5.0; 10.0; 15.0; 20.0 deg

soon as the RPA test-monitoring screen had informed the operator that the set strain was reached and apparently stable. Strain and torque signals were analyzed by Fourier transform according to the data treatment technique described above.

Results on EPDM samples

Standard considerations on strain sweep test results

Figure 7 shows test results provided by the standard data treatment of the RPA. As can be seen, the test appears fairly reproducible because the same results are obtained when testing two samples of the same material. A linear viscoelastic response, characterized by the independency on the strain amplitude of the dynamic quantities, is apparently observed up to strain angle of 1 deg (≈14% deformation) for G', of 2 deg (≈28% deformation) for tan δ, and up to 4 deg (≈56% deformation) if one considers G''. No significant differences are observed between the three materials when considering the elastic modulus, while the viscous modulus appears well affected by the long chain branching content: the lower the LCB, the higher the G″, at least in the linear viscoelastic region. One note, however, that, because the molecular weight distributions (and likely the "chain topology") of the EPDM samples are also different, one could also assign the observed differences to these material parameters.

Fourier transform rheometry approach

Using the calculation technique described above, Fourier transform was performed on all strain signals recorded during strain sweep tests with the data acquisition system. FT spectra were obtained from which the magnitude (in arbitrary units) of the main torque component, i.e., at 1 Hz, the test frequency, and the relative odd-harmonic components, i.e., the ratio $T(n\omega_1)/T(\omega_1)$, in %, where $n = 3,5,7\ldots$, were extracted. Strain sweep tests were at least repeated, and even performed on three samples of one material (G6850).

Figure 8 shows the main torque components from Fourier transform treatment of strain sweep tests on the EPDM materials. In the low strain region, a linear

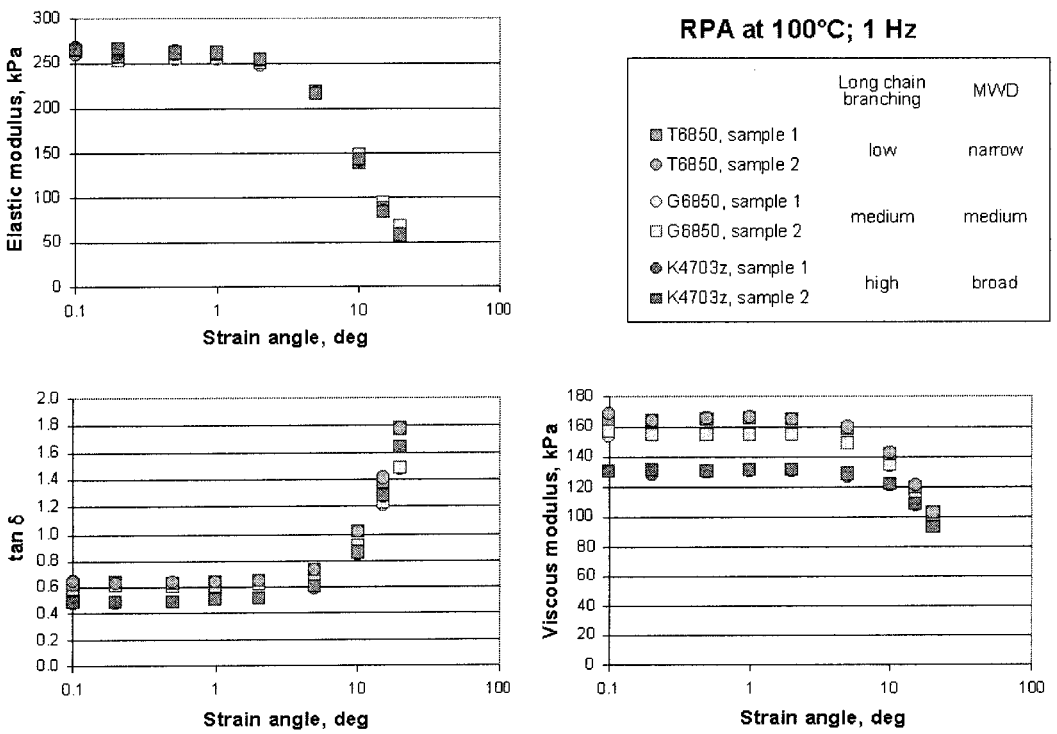

Figure 7 Strain sweep tests on EPDM samples; RPA built-in data treatment.

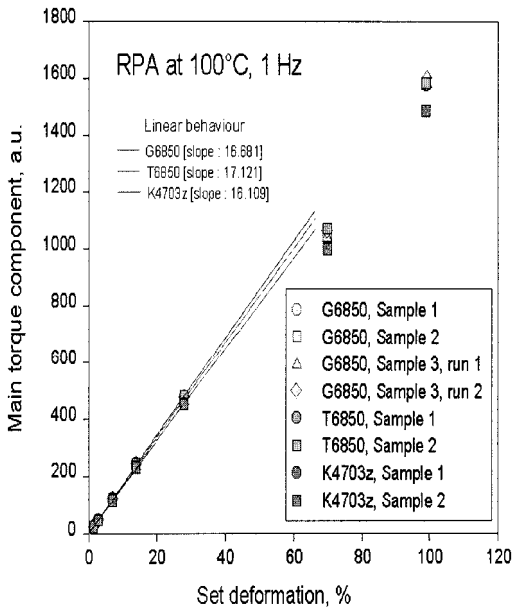

Figure 8 Main torque components from Fourier transform treatment of strain sweep tests on EPDM materials.

variation of the main torque component with the set deformation is observed, as reflected by the linear fit of the first five data points (up to 2 deg ≈ 28% deformation). Fit straight lines passes through zero and the slope depends on the elastomers, i.e., 16.68 for G6850 (r^2 = 0.9993), 17.12 for T6850 (r^2 = 0.9997) and 16.11 for K4703z (r^2 = 0.9995). This linear variation of $T(\omega_1)$ reflects obviously the linear viscoelastic behavior of the materials up to around 28% deformation and the slopes obtained by linear regression are, as expected, commensurate with the G' data, as provided by the built-in data treatment of the instrument. While small, the slope differences are significant, and likely reflects the choice of the samples series, nearly equivalent in terms of ethylene and ENB content, and of (Mooney) viscosity. Other differences, if any, that could result from the structural characteristics of the three materials must be sought in the fine information provided by the Fourier transform analysis, in other words the odd-harmonic components. By observing when the linear dependence of $T(\omega_1)$ on the deformation ceases to be obtained, an unambigeous limit of the linear viscoelastic behavior can be determined for the materials tested.

As previously described, the Fourier transform analysis was performed on the torque signals captured during the strain sweep tests. Harmonics up to $T(7\omega_1)$ or $T(9\omega_2)$ are unambiguously detected but higher ones are becoming too small to be clearly distinguished from the noise. Obviously, the higher the number of data points treated by the FT algorithm, the higher the signal-to-noise (S/N) ratio. But the required number of data points progresses by a power of 2 and the choice of 4096 points (i.e., 2^{12}) is a compromise that allows a satisfactory pertinence of the analysis, providing one considers the most intense harmonics. Wilhelm et al.[8] have demonstrated that the envelope function for the intensity of the different harmonics decreases as $1/n\omega_1$, where n = 3, 5, 7. In other words, the limit of the relative torque harmonic $T(n\omega_1)/T(\omega_1)$ is expected to be equal to $1/n$, if both infinite high torques and a shear rate-dependent viscosity are considered. Consequently $T(3\omega_1)/T(\omega_1)$ is the most intense contribution compared to all other harmonics. As shown in Figure 9, for the Buna EP T6850 material, this is indeed the case, and similar figures are obtained with the other EPDM samples tested. The third and the fifth relative harmonic components can clearly be detected and, as expected, their intensity is increasing with the strain angle. At low strain angle, there is some scatter that is discussed hereafter.

Relative third harmonic components at all strain angles tested are given in Table V. All materials were tested twice, G6850 three times, and for this material the results of two successive runs (on the same sample; see test protocol described above) are also given. Except at low strain angle (i.e., ≤0.5 deg; ≈7% deformation), the results are well reproducible, and no significant sample effect is seen.

Let us consider the variation of the relative third harmonic component with the strain amplitude. Figure 10 shows test results obtained on all samples. As can be seen, an S-shape variation is observed, from a (scattered) plateau value at low strain up to a maximum at high strain. The insert is a magnification of the low strain data by using a logarithmic scale for the strain angle; no clear sample or material effect is observed when the set strain is lower than 5 deg.

Wilhelm et al.[3] attempted to describe the variation of the third harmonic component with the following equation:

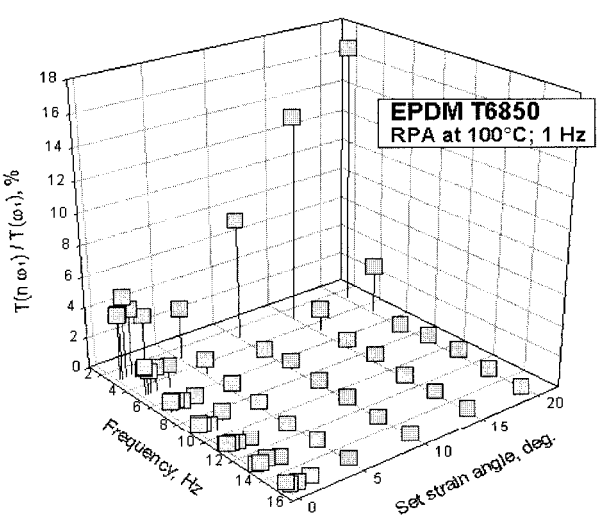

Figure 9 Relative harmonic components from Fourier transform analysis of strain sweep test data.

TABLE V
Third Relative Harmonic Components vs. Set Strain Angle

Material:	T6850		G6850				K4703Z	
Sample:	1	2	1	2	3 Run 1	3 Run 2	1	2
Set strain deg	$\frac{T(3\omega_1)}{T(\omega_1)}$ %	$\frac{T(3\omega_1)}{T(\omega_1)}$ %	$\frac{T(3\omega_1)}{T(\omega_1)}$ %	$\frac{T(3\omega_1)}{T(\omega_1)}$ %	$\frac{T(3\omega_1)}{T(\omega_1)}$ %	$\frac{T(3\omega_1)}{T(\omega_1)}$ %	$\frac{T(3\omega_1)}{T(\omega_1)}$ %	$\frac{T(3\omega_1)}{T(\omega_1)}$ %
0.1	4.467	4.267	3.004	3.877	1.153	8.457	5.365	4.045
0.2	4.514	4.236	2.625	5.472	3.956	6.279	4.256	4.290
0.5	5.277	5.630	4.120	5.938	3.590	5.388	5.325	5.305
1.0	4.272	4.613	4.124	4.842	3.133	3.892	4.144	3.990
2.0	3.714	3.831	3.316	3.738	3.354	3.413	3.686	3.721
5.0	3.352	3.428	3.266	3.352	3.243	3.373	3.461	3.453
10.0	8.118	7.783	5.730	6.047	6.229	6.258	6.256	6.223
15.0	13.370	13.610	10.770	10.790	10.610	10.670	10.710	10.510
20.0	16.940	17.050	12.610	12.760	12.620	12.660	13.860	13.610

$$I_{3/1} = A\left[1 - \exp\left(\frac{\gamma_0 - \gamma_L}{k}\right)\right] \quad (1)$$

where $I_{3/1}$ stands for the relative third harmonic component [i.e., $T(3\omega_1)/T(\omega_1)$ in our formalism], A is the maximum possible third harmonic contribution at an idealized infinite shear amplitude, γ_0 the applied strain amplitude, γ_L the maximum shear amplitude within the concept of a linear response regime, and k a parameter that describes the relative intensity change of the third harmonic with γ_0 (in fact, the inverse slope). Obviously, γ_0 must be higher than γ_L, and the curve should intercept the strain axis at γ_L. Wilhelm,[1] when performing very low shear experiments at 0.1 Hz on a polyisobutylene solution, showed that even for very small strain amplitudes, nonlinear contributions could still be detected via the third harmonic contributions, while fitting eq. (1) to experimental data yielded $\gamma_L = 0.64$. No crossover to a linear regime could be detected experimentally in the very low shear amplitude region.

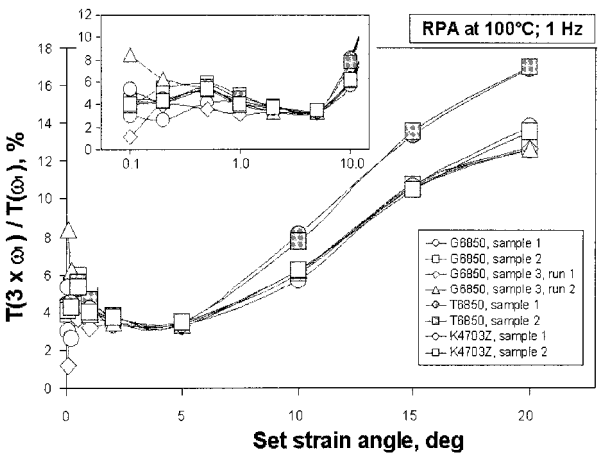

Figure 10 Relative third harmonic component vs. strain amplitude; all EPDM samples.

Figure 10 clearly suggests that a sigmoidal type of equation would be appropriate to meet experimental observations. The following model was, therefore, considered:

$$\left[\frac{T(3\omega_1)}{T(\omega_1)}\right]_\gamma = \left[\frac{T(3\omega_1)}{T(\omega_1)}\right]_{\min} + \left\{\left[\frac{T(3\omega_1)}{T(\omega_1)}\right]_{\max} - \left[\frac{T(3\omega_1)}{T(\omega_1)}\right]_{\min}\right\} \times [1 - \exp(-b\gamma)]^c \quad (2)$$

where

$$\left[\frac{T(3\omega_1)}{T(\omega_1)}\right]_{\min} \text{ and } \left[\frac{T(3\omega_1)}{T(\omega_1)}\right]_{\max}$$

are the limiting third harmonic components at very low and very high (infinite) strain, respectively, γ the strain amplitude, b and c fit parameters. Figure 11 shows how this equation fits (by nonlinear regression) G6850 samples data.

Similar graphs are obtained with the other EPDM samples, and the corresponding fit parameters are given in Table VI.

At first glance, the minimum third harmonic component appears to depend on the material tested, but this parameter describes the curve in the data range where the scatter is maximum. When considering the quality of the applied strain signal (see previous), it was noted that the scatter on $S(3\omega_1)/S(\omega_1)$ started to reduce when set strain is higher than 0.5 deg, with an erratic large scatter below this strain angle. It is, therefore, attractive to consider that there is a minimum third harmonic component for the torque, i.e., $T(3\omega_1)/T(\omega_1)$, in the same range, let's say 3.5%, irrespective of

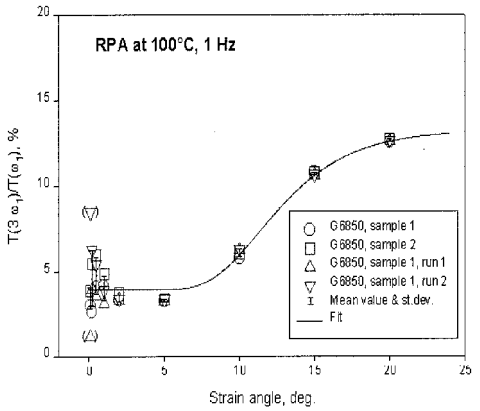

Figure 11 Relative third harmonic component vs. strain amplitude; G6850 samples; fit without constraint on parameters.

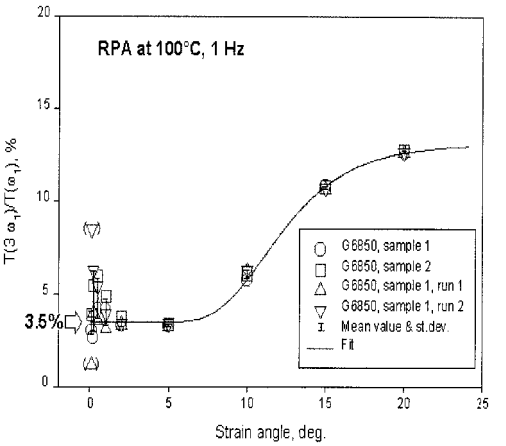

Figure 12 Relative third harmonic component vs. strain amplitude; G6850 samples; fit with a constraint (= 3.5%) on the minimum third harmonic contribution parameter.

the material tested. Equation (2) was consequently fit again on experimental data but with the constraint that the parameter

$$\left[\frac{T(3\omega_1)}{T(\omega_1)}\right]_{\min}$$

is constant and equal to 3.5. Figures (12) to (14) show the results of such a data treatment, whose fit parameters are given in Table VII.

By blocking the minimum contribution parameter, the scatter in the low strain region is completely ignored and the curve fit is clearly better. There are obviously some effects on the values of the other parameter but without introducing any change in the comparison between the three materials. Differences in the maximum third harmonic contribution and in parameters b and c are seen, but without clear ranking with respect to the long branching content of the materials. For instance, T6850, which has the lowest degree of LCB, exhibits the highest maximum third harmonic component. One would, therefore, expect a strong nonlinear behavior for this material, which is indeed the case as reflected by the $\Delta\delta$ value (see Table III). But the two other materials have $T(3/1)_{\max}$ values that do not rank according to either the LCB degree or the $\Delta\delta$ parameter. Limper and Keuter[9] used the same series of EPDM materials to study the effect of long chain branching on mixing behavior. They observed that the specific mixing energy of the crumbling phase of the highly branched polymer K4703z was lower in comparison to the other polymers. They explained this unexpected result by showing that this material contains twice more processing aids (likely zinc stearate, plus some magnesium components) than the two other EPDMs. Such additives are indeed used by polymer manufacturers to compensate, or at least limit, the trend to self-shrink of long branched polymers. It would, therefore, be quite remarkable that Fourier transform rheometry has the capability to detect such effects, not appearing in the standard dynamic tests on which the $\Delta\delta$ method is based.

How the relative third harmonic component varies with the strain amplitude is determined by the two parameters b and c, for which there is no clear meaning at this stage, except their mathematical virtue.

TABLE VI
Effect of Strain Amplitude on Third Harmonic Component; Fit Parameters Obtained by Nonlinear Regression of Eq. (2)

Material	T6850	G6850	K4703z
$T(3/1)_{\min}$	4.30	3.92	4.26
$T(3/1)_{\max}$	18.79	13.28	15.73
b	0.230	0.300	0.220
c	13.40	30.00	15.00
r^2	0.986	0.979	0.977

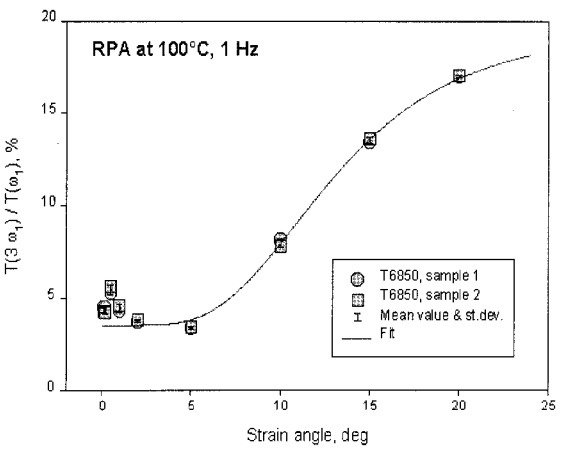

Figure 13 Relative third harmonic component vs. strain amplitude; GT850 samples; fit with a constraint (= 3.5%) on the minimum third harmonic contribution parameter.

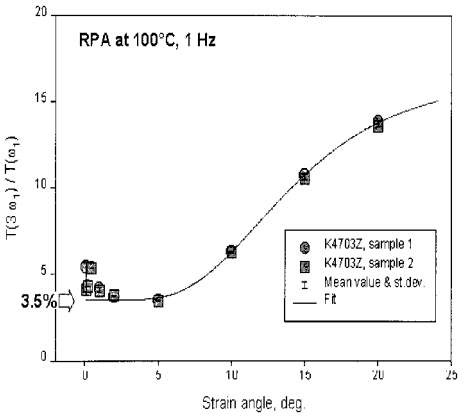

Figure 14 Relative third harmonic component vs. strain amplitude; K4703z samples; fit with a constraint (= 3.5%) on the minimum third harmonic contribution parameter.

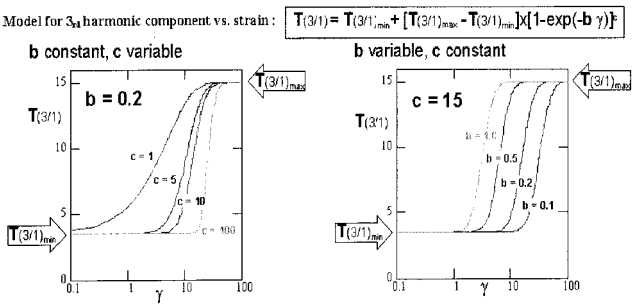

Figure 15 Model for third harmonic component variation with strain amplitude.

Indeed, as illustrated in Figure 15, b and c affect the shape on the curve in quite a complex manner. At constant b, the lower c, the smoother the transition from $T(3/1)_{min}$ to $T(3/1)_{max}$; at constant c, the lower b, the longer the delay before $T(3/1)$ starts to significantly increases with strain. In a sense, the parameter b could be viewed as indicating the transition towards a strong nonlinear behavior. Another manner to approach the physical meaning of parameters b and c would be to consider b as proportional to a "pivot point" and to relate c with the slope at this pivot point. Then, with respect to the large strain amplitude applied, parameter b might be related to extensional properties, for instance, the extensional thickening response in elongational rheometry. What such observations exactly mean in terms of material characteristics must be addressed in further works, with materials well defined in terms of macromolecular dimensions and polymer architecture.

TESTING GUM SBR 1500 THROUGH FT RHEOMETRY

SBR test materials

Styrene–butadiene rubbers are the backbone of the synthetic rubber industry with a world-wide consumption in the 3.7 10^6 tons range in 2002.[10] Emulsion SBR 1500 is likely the most common grade because its properties are designed to match Natural Rubber as closely as possible. Properly speaking however, there is no precise specification for SBR 1500, but most manufacturers would agree with the range of properties described in Table VIII.[11]

Virtually, there is no standardization on SBR 1500, which is currently sold as a commodity material but is not produced as a commodity because all suppliers produce many grades to meet the demand by different tyre makers. A good-quality SBR 1500 is expected to exhibit the following characteristics (Table IX).

To assess the capabilities of FT rheometry to detect differences between rubber materials that are considered as belonging to the same type, a series of SBR 1500 samples from different suppliers was collected, either directly through their local representatives or via some of their customers. Several kilogrammes samples were obtained, wrapped in plastic film and stored in darkness below 0°C. Samples are described in Table X, with their code names and corresponding characteristics (suppliers data)

TABLE VII
Effect of Strain Amplitude on Third Harmonic Component; Fit Parameters Obtained by Nonlinear Regression of Eq. (2) with a Constraint on the Minimum Third Harmonic Contribution

Material	T6850	G6850	K4703z
$T(3/1)_{min}$	3.50	3.50	3.50
$T(3/1)_{max}$	19.19	13.11	16.28
b	0.200	0.330	0.190
c	8.74	38.29	9.33
r^2	0.968	0.983	0.944

RPA test protocols

Using an 18-mm diameter die, test samples of circular cross-section were cut out of 2 cm-thick slices. Each sample was weighed and, if necessary, adjusted in order to maintain its weight within 3.05 ± 0.4 g.

TABLE VIII
General Properties of SBR 1500

Polymerization type	Emulsion
Styrene level, % weight	23–40
Vinyl level, % weight	15–20
Styrene distribution	random
Max. fatty acid content, % weight	6
Molecular weight	uncontrolled
Molecular weight distribution	broad
Long chain branching	appreciable
Antidegradant	staining
Mooney viscosity, $ML(1 + 4)_{100°C}$	45–55

TABLE IX
SBR 1500 Macromolecular and Other Characteristics

Property		Range
Styrene content, (%)		23.5 ± 0.5
Butadiene structure	Vinyl (%)	16 ± 1
	cis-1,4 (%)	12 ± 1
	trans-1,4 (%)	72 ± 1
Glass transition temperature, Tg (°C)		−50 ± 5
Density		0.94 ± 0.01
Molecular weight	Weight average M_w (g/mol)	400,000 ± 20,000
	Number average M_n (g/mol)	78,000 ± 2000
Free soap (%)		0.5 max

Strain sweep tests were performed with the RPA, according to the protocol previously described (see earlier), with the data acquisition activated at each strain step to record 10,240 points at the rate of 512 pt/s. Elastic and viscous moduli assessed through the standard data treatment of the instrument were simultaneously collected. Strain and torque signals were analyzed by Fourier transform according to the data treatment technique described above.

Results on SBR 1500 samples

Standard test results from strain sweep experiments

Figure 16 shows elastic modulus results provided by the standard data treatment of the RPA. Mean data from four tests (two samples with two succesive runs each) are plotted with the standard deviation. As can be seen, all SBR 1500 samples exhibit a linear viscoelastic plateau up to around 1 deg strain angle (≈14% deformation), but the plateau modulus values are significantly different, within a 50-kPa range. The extend of the linear region is indicated by the dashed area. Except for Iw1500, modulus measurements are well reproducible, within the kPa range. The ±10-kPa scatter observed with Iw1500 likely reflects the poor quality of this material, which, however, exhibits, the highest average G' in the linear region, as shown by the inserted bar graph. The reprocessed material (Um1500) has also a higher elastic modulus, but result reproducibility is comparable to virgin materials. One notes that, with respect to the elastic modulus, three materials appear very close, i.e., Bn1500, Bu1500, and Kx1500.

When considering the viscous modulus data (Fig. 17), a longer viscoelastic plateau is observed, clearly up to 2 deg strain angle (dashed area). Individual data scatter is negligible for all samples but abnormal G'' values are sometimes obtained at the lowest strain angle considered. Again all those SBR 1500, materials appears significantly different with respect to their G″ in the linear region within a 20 kPa range. Three materials exhibit very close viscous moduli, Bn1500, Bu1500 and In1500. It is worth underlining that only Bn1500 and Bu1500 have nearly similar elastic and viscous moduli, but this was somewhat expected since those samples are from the same supplier (but likely not from the same plant).

Fourier transform rheometry approach

Fourier transform was performed on strain signals recorded during strain sweep tests on SBR materials. Each material was first tested at least twice (on different samples), with two successive strain sweep tests, as previously described in Table IV, and the higher strain range was further investigated with another sample, submitted to two successive high strain sweep tests, as described in Table XI. Note that a 30 deg strain angle is the maximum deformation (≈419%) permitted at 1 Hz with the RPA. FT spectra were obtained from which the magnitude (in arbitrary units) of the main torque component, i.e., at 1 Hz, the test fre-

TABLE X
SBR 1500 Samples

Sample code	Supplier	SBR type	Mooney ML (1 + 4) 100°C	Styrene content (%)	Organic acid (%)
Kx1500	A	emulsion	44–54	22.5–24.5	n.a.
Bu1500	B	emulsion	52 ± 5	23.4 ± 0.9	6.4 ± 0.5
Bn1500	B	emulsion	50 ± 5	23.5 ± 1.0	6.5 ± 0.6
Iw1500	C	emulsion	45–55	n.a.	n.a.
In1500	D	emulsion	52 ± 5	23.5 ± 1.0	n.a.
Kr1500	E	emulsion	46–54	22–25	5.0–7.5
Um1500	F	reprocessed E-SBR	25–55	23.5	n.a.

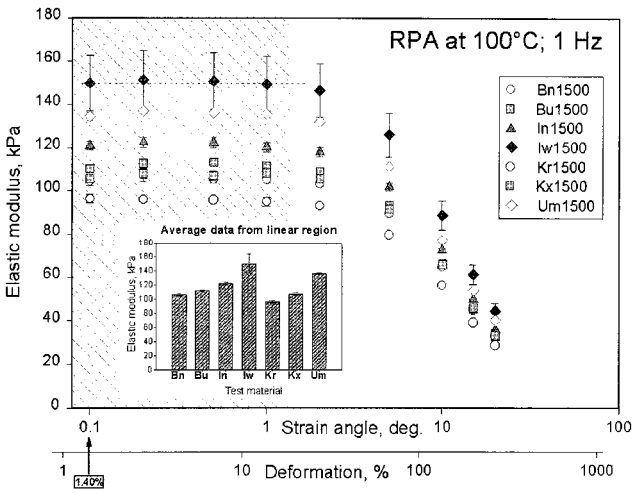

Figure 16 Elastic modulus from strain sweep tests on SBR 1500 samples; RPA built-in data treatment.

quency, and the relative odd-harmonic components, i.e., the ratio $T(n\omega_1)/T(\omega_1)$, in %, where $n = 3, 5, 7, \ldots$, were extracted.

Figures 18 and 19 show the relative third harmonic component as measured on Bn1500 and Bu1500 samples. Lower strain angle data are scattered, in agreement with a similar observation made on gum EPDM samples. With respect to the lower quality of the applied strain signal below 0.5 deg (see earlier), no particular meaning would be assigned to this observation, but it is striking to see that the scatter reduces as the strain angle increases to eventually reach a remarkable reproducibility above 1 deg strain. Expressing the strain angle on a logarithmic scale clearly illustrates this point (see inserts in Figs. 18 and 19). Similar observations are made with all the other SBR1500 materials.

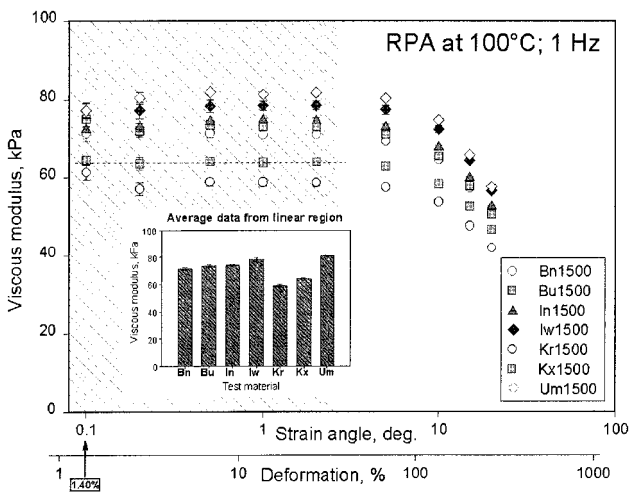

Figure 17 Viscous modulus from strain sweep tests on SBR 1500 samples; RPA built-in data treatment.

TABLE XI
RPA; Strain Sweep Test Protocol

RPA test conditions	Temp. (°C): 100 Freq. (Hz): 1
Sample conditionning	
Preheating	3 min, at rest
Fixing	30 sec; 1 Hz; 0.05 deg.
Strain sweep test (run 1)	
Dwell time	2 min, at rest
Strain Sweep	10.0; 20.0; 25.0; 30.0 deg
Strain sweep test (run 2)	
Dwell time	2 min, at rest
Strain Sweep	10.0; 20.0; 25.0; 30.0 deg

Qualitatively, all SBR 1500 samples exhibit thus the same variation upon strain of the relative third harmonic component, but the minimum $T(3/1)$ ratio seems slightly different, as well as the slope of the curve, and the $T(3/1)$ ratio at high strain appears to depend on the origin of the sample. This suggests obviously that eq. (2) could also be used to fit the results. Figure 20 shows how the model meets the (mean) data obtained with sample In15000, either by fixing the minimal $T(3/1)$ contribution equal to 3% or by letting the nonlinear algorythm to fit $T(3/1)_{min}$. In agreement with the comments earlier, scattered data in the low strain region were not considered in the fitting process. As can be seen, fixing or not $T(3/1)_{min}$ does not produce significant differences, and the same observation is made with all the other samples, except sample Kx1500 (see Fig. 21)

Fixing or not $T(3/1)_{min}$ in fitting eq. (2) to experimental results depends on whether or not one considers that low strain data loose significance below 1.0 deg strain angle or that the so-called linear viscoelastic response would be characterized by a constant (but not zero) third harmonic contribution. It is misfortunate that below 1.0 deg the quality of the strain signal applied by the RPA is deteriorating as the strain mag-

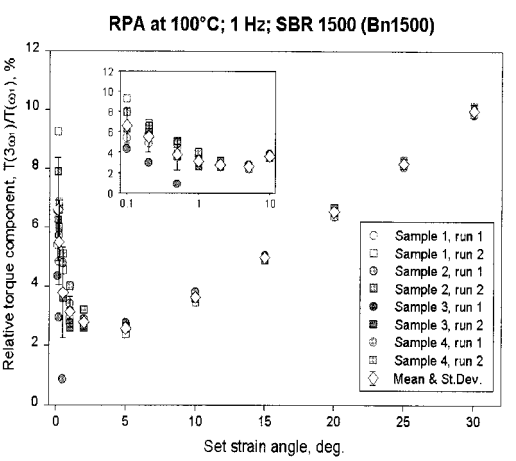

Figure 18 Fourier transform rheometry on SBR sample (Bn1500); relative third harmonic component.

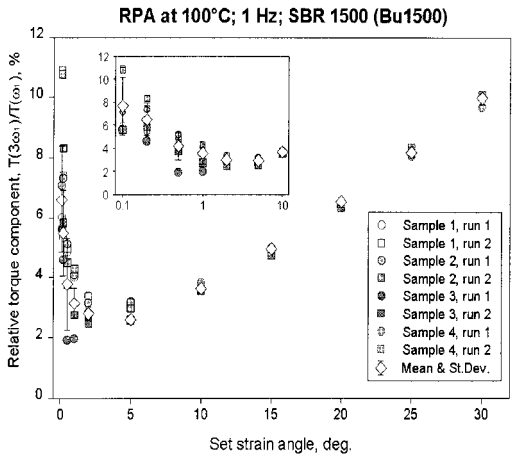

Figure 19 Fourier transform rheometry on SBR sample (Bu1500); relative third harmonic component.

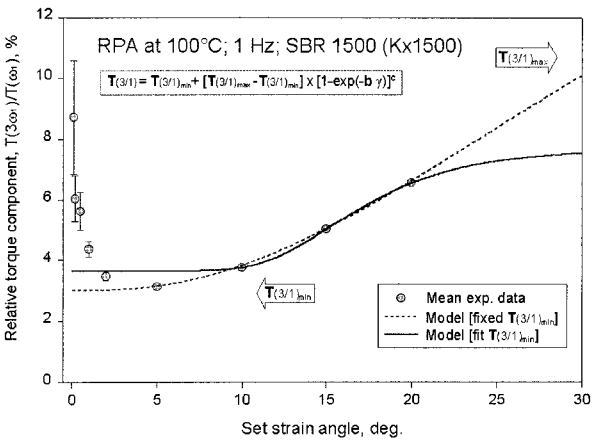

Figure 21 Relative third harmonic component vs. strain amplitude; Kx1500 samples; fit either without or with a constraint (= 3.0%) on the minimum third harmonic contribution parameter.

nitude decreases (as clearly shown in Fig. 4). But all the data obtained suggest that, whatever the tested materials, the relative third harmonic component is never going to zero as the strain magnitude decreases but tends towards a constant value (in the 3.0–3.5% range), unfortunately hidden by the limits of the test device in the (very) low-strain region. A similar observation was made by Wilhelm[1] when testing a polyisobutylene solution at 0.1 Hz. Even for very small shear amplitudes, he detected a nonlinear contribution via the third harmonic component and never observed any crossover from a nonlinear to a linear regime. But "while far reaching in rheology, the linear response is by itself only a concept," Wilhelm commented. If, indeed, the so-called linear regime of a given polymer is characterized, not by $T(3/1)_{min} = 0$, as implicit in the strict proportionality expected between strain and torque signals, but by a constant relative third harmonic component (whose value would depend on the material), then Fourier transform data fitted with eq. (2) would easily give access to this material parameter. Figure 21 somewhat supports this view because the fit is clearly better when $T(3/1)_{min}$ is considered as a fit parameter.

Figure 22 shows the results obtained with all the SBR 1500 samples investigated, when fitting the relative third torque component vs. strain with eq. (2). The corresponding values of the fit parameters are given in Table 12.

Figure 22 shows all the SBR 1500 samples exhibit a nonlinear viscoelastic response with the same qualitative features, but with respect to the magnitude of $T(3/1)$ at 30 deg strain, one can split them into three groups: Um, Kr, and Kx, then the others. The fit parameters, particularly b and c, allow the differences between the materials to be seen in a more precise manner. High b and c values would mean that the nonlinear viscoelastic character increases faster when

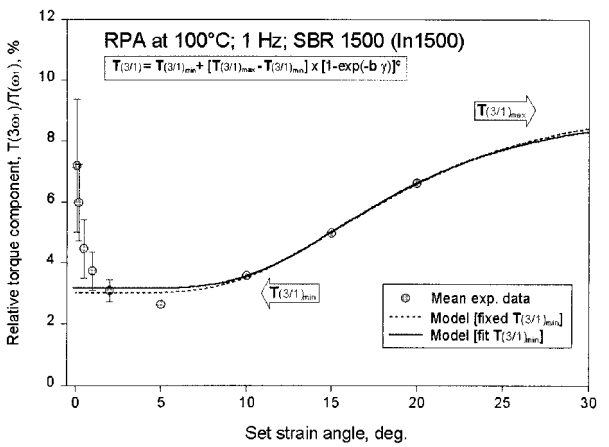

Figure 20 Relative third harmonic component vs. strain amplitude; In1500 samples; fit either without or with a constraint (= 3.0%) on the minimum third harmonic contribution parameter.

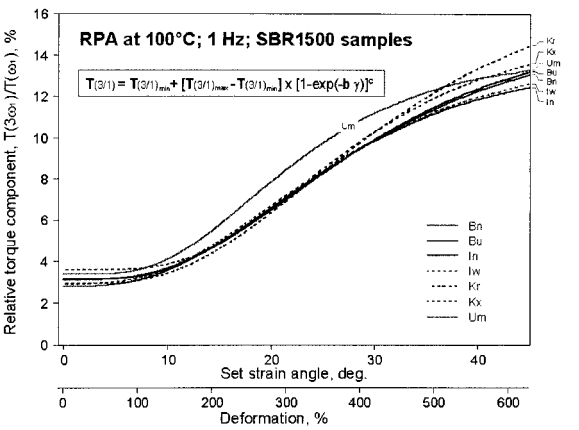

Figure 22 Relative third harmonic component vs. strain amplitude; SBR 1500 samples; fit without constraint on the minimum third harmonic contribution parameter.

TABLE XII
Effect of Strain Amplitude on Third Harmonic Component; Fit Parameters Obtained by Nonlinear Regression of Eq. (2)

SBR 1500	$T(3/1)_{min}$	$T(3/1)_{max}$	b	c	r^2
Bn	2.83	15.54	0.065	3.85	0.982
Bu	3.16	15.51	0.070	4.63	0.952
In	3.15	13.79	0.083	5.36	0.967
Iw	2.97	14.25	0.075	4.39	0.979
Kr	2.95	17.85	0.065	4.65	0.966
Kx	3.61	15.22	0.085	6.83	0.955
Um	3.40	14.02	0.099	5.85	0.984

the strain amplitude increases. This is clearly the case of Kr and Kx samples, which, however, were exhibiting the lowest G' and G'' values in the standard (linear) dynamic tests (see Figs. 16 and 17). The highest G' and G'' values measured on Iw1500 do not reflect in the relative third harmonic component of this material which, through Fourier transform rheometry, appears to exhibit the same nonlinear behaviour as In1500. Samples Bu and Bn, despite some differences in the fit parameters, have the same nonlinear behavior, as expected for materials from the same supplier.

CONCLUSIONS

Fourier transform rheometry is a powerful technique to investigate the viscoelastic behavior of polymers and, by instrumenting a torsional dynamic rheometer, especially designed to easily test stiff rubber materials, reproducible results are obtained. Like any other method, FT rheometry requires a careful selection of test conditions, an adequate protocole for the data acquisition and the appropriate calculation technique. When compared to standard harmonic testing, FT rheometry offers the advantage that no condition must be fullfilled in terms of strain amplitude, because the method is valid in both the linear and nonlinear viscoelastic domains. Fourier transform spectra contain obviously more information that G' and G'' data from linear dynamic testing. The main torque component (i.e., the first harmonic) is commensurate with the complex modulus, and within the linear domain does not likely provide more than the latter, except may be an easier detection of the departure from the linear behavior, when a strict proportionality between $T(\omega_1)$ and set strain ceases to be observed. The real interest of FT rheometry resides in the higher harmonics in the torque signal, whose intensity increases with the applied strain, and the relative third harmonic is found large enough to be significantly measured with minimum care in the testing protocol.

The polymer structure affects the dependence upon strain of the relative third harmonic component, which is adequately modeled with a simple four parameters model. However, results with three EPDM samples with claimed different LCB content do not fully meet expectation, likely because one of the sample contains a higher amount of processing aid. In this respect, Fourier transform rheometry appears as very sensitive to the presence of additives in gum elastomers. The four parameters model found very efficient in fitting $T(3\omega_1)/T(\omega_1)$ ratio vs. strain shows that the relative third harmonic component does not vanished when the deformation goes to zero but plateaus out towards a value in the 3–4% range of the main harmonic component. Below the 0.5 deg strain (≈7% deformation), a large scatter is observed on $T(3/1)$ data from Fourier transform, and the plateauing out might be due the a lack of sensitivity of the dynamic rheometer in the low strain region. However, this behavior was observed with all gum elastomers tested (three EPDM, seven SBR) and the hypothesis that the linear behavior of polymers is characterized not by the absence of any higher harmonics but by a constant level of $T(3\omega_1)/T(\omega_1)$, in the 3–4% range, must be considered carefully.

The capability to detect differences in a series of SBR 1500 from different manufacturers calls for further works but can be considered as a strong demonstration of the possibilities of FT rheometry.

References

1. Wilhelm, M. Macromol Mater Eng 2002, 287, 83.
2. Leblanc, J. L.; de la Chapelle, C. Rubber Chem Technol 2003 (in press).
3. Wilhelm, M.; Reinheimer, P.; Ortseifer, M. Rheol Acta 1999, 38, 349.
4. Macosco, C. W. Rheology Principles, Measurements and Applications; VCH, Wiley: New York, 1994.
5. Leblanc, J. L.; Mongruel, A. Prog Rubber Plast Technol 2001, 17, 162.
6. Nelson, B. I.; Dealy J. M. In Rheological Measurements; A. A. Collyer, D. W. Clegg, Eds; Chapman & Hall: London, 1998, p. 138, Chap. 4, 2nd ed.
7. Booij H. J. Kautsch Gummi Kunstst 1991, 2, 128.
8. Wilhelm, M.; Maring, D.; Speiss H. W. Rheol Acta 1998, 37, 399.
9. Limper, A.; Kauter H. Intern. Conf. "A Review of European Rubber Research in Practice," Paderborn, Germany, January 9–10, 2002, p. 163.
10. Rubber World, 2001, 224, 18.
11. Source: Manual for the Rubber Industry; Bayer: Leverkusen, Germany, 1993, 2^{d} ed.